solids

MDPI

Article

Interplay Between Structural, Electronic, and Magnetic Properties in the d^0-d Semi-Heusler Compounds; the Case of the K-Based Compounds

Kemal Özdoğan [1,†] and Iosif Galanakis [2,*,†]

[1] Department of Physics, Yildiz Technical University, 34210 Istanbul, Turkey; kozdogan@yildiz.edu.tr
[2] Department of Materials Science, School of Natural Sciences, University of Patras, GR-26504 Patra, Greece
* Correspondence: galanakis@upatras.gr
† These authors contributed equally to this work.

Abstract: Heusler compounds and alloys represent a rapidly expanding family of materials that exhibit novel properties of significant interest for advanced technological applications. Electronic band structure calculations play a pivotal role in advancing research in this area. In an earlier study, we explored the properties of a new class of Heusler compounds based on Li, referred to as "p^0-d semi-Heusler Compounds". In this study, we take the research a step further by focusing on "d^0-d semi-Heusler Compounds", with the chemical formula KZ(Ga, Ge, As, or Se), where Z represents a transition metal. Our investigation centers on the structural, electronic, and magnetic properties of these compounds, particularly in relation to the three possible $C1_b$ structures. Most of these compounds are found to be magnetic and, notably, several among them exhibit half-metallicity making them appealing for applications in spintronics. Our findings provide a foundation for future experimental research on these materials.

Keywords: Heusler compounds; *ab initio* calculations; electronic structure; magnetic materials; Slater–Pauling rule

Citation: Özdoğan, K.; Galanakis, I. Interplay Between Structural, Electronic, and Magnetic Properties in the d^0-d Semi-Heusler Compounds; the Case of the K-Based Compounds. *Solids* **2024**, *5*, 533–543. https://doi.org/10.3390/solids5040036

Academic Editor: Antonio Polimeni

Received: 10 September 2024
Revised: 14 October 2024
Accepted: 4 November 2024
Published: 7 November 2024

1. Introduction

In the early 20th century, German metallurgist Heusler made a significant breakthrough while researching ways to improve the electrical conductivity of steel [1,2]. He discovered a novel compound, Cu_2MnAl. As scientific instruments advanced over the decades, it was revealed that Cu_2MnAl has a face-centered cubic (f.c.c.) lattice structure, which is similar to well-known semiconductors like Si and GaAs. This same structure was later identified in various intermetallic compounds with unique properties, which became known as "Heusler compounds" or "Heusler alloys" [3–5]. Heusler compounds can be categorized into four main families based on their atomic composition and valence: (a) semi-Heusler (or half- Heusler) compounds, like NiMnSb, crystallizing in the "$C1_b$" structure; (b) full-Heusler compounds, such as Co_2MnSi, crystallizing in the "$L2_1$" structure; (c) inverse Heuslers resemble full-Heuslers, like Mn_2CoSi with their structure designated as "XA" or "$X\alpha$"; and (d) ordered equiatomic quaternary Heusler compounds, such as (CoFe)TiSi crystallizing in the "LiMgPdSn" structure [4,6]. A few among them are ferromagnetic with high Curie temperatures. Recently, there has been growing interest in Heusler compounds containing exclusively transition metal atoms, which are known as all-d-metal Heusler compounds [7–10].

One of the key properties of Heusler compounds is the so-called half-metallicity [11]. Half-metallic ferro- or ferri-magnetic materials exhibit metallic behavior for majority spin electrons while acting as semiconductors for minority spin electrons [12]. This results in high spin polarization at the Fermi level, making them highly attractive for spintronics and magnetoelectronics, with the potential to enable novel electronic device functionalities.

Heusler compounds have the advantage of combining their half-metallic character with high values of their Curie temperatures and thus have attracted strong interest due to their potential applications [13–16].

First-principles (or *ab initio*) calculations have emerged as a powerful tool for understanding material properties and predicting new compounds with tailored characteristics; e.g., spin-gapless semiconducting and spin-filtering behaviors [17]. In recent years, several large databases based on first-principles calculations have been created, covering hundreds of magnetic Heusler compounds [18–24]. These databases complement more focused studies that investigate the fundamental properties of specific Heusler compounds. In magnetic semi-Heusler compounds having the chemical formula XYZ, X is typically a transition metal or rare-earth element. However, in semi-Heusler compounds, X can sometimes be replaced by an alkali or alkaline-earth metal, leading to the formation of "p^0-d" or "d^0-d" Heusler compounds. The term p^0 refers to elements like Li, Be, Na, and Mg, while d^0 refers to elements such as K, Rb, Cs, Ca, Sr, and Ba, reflecting the nature of the first unoccupied states in the free atom.

Damewood et al. [25] and Dehghan and Davatolhagh [26] conducted ab initio studies on compounds like LiMnPt, SrVSb, and KMnP. In 2022, Shakil and collaborators studied the KMn(B, Si, Ge, As) compounds also using first-principles calculations and assuming a cubic lattice structure [27]. In Reference [28], Dehghan and Davatolhagh developed a database of 420 XYZ d^0-d Heusler compounds, where X is K, Rb, or Cs, Y is a transition metal, and Z is a group-IV, -V, or -VI element. Of these, 98 were identified as half-metals, following the Slater–Pauling rule: $M_t = Z_t - 8$ (or $M_t = Z_t - 18$ when Y is Cu or Zn) [11]. In 2022, the same group expanded their database to include p^0-d semi-Heusler compounds, where X is Li, Be, Na, or Mg, and Z is a group-V or group-VI element [29]. While these databases offer valuable insights into a wide range of compounds, they do not delve into the detailed properties of individual compounds. Consequently, we have presented in Reference [30] a detailed study of the structural, electronic, and magnetic properties of the LiYGa and LiYGe compounds, where Y is a 3d transition metal, and their interconnection. Our study revealed that these compounds do not crystallize in the usual α variant of the $C1_b$ structure and there are a few compounds which are half-metals for all three possible variants of this structure.

2. Materials and Methods

In the present study, we expand our work on the Li-compounds, to the case of the d^0-d Heusler compounds. As representative families we have chosen the KZGa, KZGe, KZAs, and KZSe compounds where Z varies between Sc and Zn. Such a choice enables us to investigate the effect not only of the Z element but also of the sp elements on the properties of these compounds. For our first-principles electronic band structure calculations, we employed the full-potential nonorthogonal local-orbital minimum-basis band structure approach (FPLO) (version FPLO14.00-47) [31,32] in conjunction with the Perdew–Burke–Ernzerhof (PBE) parameterization to the generalized gradient approximation (GGA) [33]. The computational details of our calculations are identical to the ones in Reference [30]. Here, we should note that GGA-PBE is known to reproduce with accuracy the properties of half-metallic Heusler compounds with respect to more elaborated meta-GGA functionals [34].

3. Results and Discussion

3.1. Structural Properties

Semi-Heusler compounds, like those studied here, crystallize in the $C1_b$ cubic lattice structure [3,4]. There is a reference dating from 1974, where authors claim that KMnAs crystallizes in a tetragonal structure [35], but no other experimental work exists on the compounds under study. As shown in Figure 1 of Reference [30], the $C1_b$ structure consists of four sites, with one site remaining vacant. Depending on the specific arrangement of the atoms, the structure can exist in three distinct variants, commonly referred to as the α,

β, and γ phases. The key difference between these phases lies in the chemical nature of the neighboring atoms, which significantly affects the orbital interactions between nearest neighbors. As a result, the physical properties of the same compound can vary greatly across these phases, despite the preservation of the overall tetrahedral symmetry. We should note that in Reference [27], the KMnGe and KMnAs compounds were studied assuming the same crystal structure as in our study. The authors found that the equilibrium lattice was the so-called type-3 structure, which corresponds to the β variant assumed in our calculations and which is also the ground state in our case as discussed below.

In Table 1, we present the structural properties for all the compounds analyzed in this study. To determine the equilibrium lattice parameter for each compound and for all three phases, we conducted total energy calculations across a wide range of lattice parameters, with the equilibrium value being the one that minimizes the total energy. The calculated equilibrium lattice constants range from approximately 6.5 Å to 7.5 Å, which is consistent with other Heusler compounds and semiconductors [3,4], and is an important factor for applications involving multilayer heterostructures. In most cases, the lattice constants follow the general trend of the atomic radii. Specifically, the atomic radii slightly decrease as we move from Ga $\rightarrow$ Ge $\rightarrow$ As $\rightarrow$ Se in the periodic table. Similarly, among the 3*d* transition metals, the atomic radii decrease progressively from Sc to V. This pattern also appeared in the case of the Li-based p^0-*d* compounds discussed in Reference [30]. However, a notable difference arises when comparing the Li-based and K-based compounds. For the Li compounds in Reference [30], the α phase generally had the smallest equilibrium lattice constants, while no consistent trend emerged between the β and γ phases—though the β phase typically had the larger constants. In contrast, for the K-based compounds, the α phase consistently exhibits the largest lattice constant, except in the cases of KScGa and KScGe. The origin of this differing behavior is difficult to pinpoint, as both the chemical composition and the magnetic properties of the compounds significantly affect the lattice constants (magnetic and non-magnetic phases of the same compound often exhibit different equilibrium lattice constants) [36].

Table 1. We provide the equilibrium lattice constants for all compounds under study in all three α, β, and γ phases. The next three columns present the total energy difference between the two phases using for each one the equilibrium lattice constant. In the last two columns, the most and least stable phases are depicted.

Compound	Lattice Constant a in Å			Energy Difference ΔE in eV			Most Stable	Least Stable
	α-Phase	β-Phase	γ-Phase	$E_\beta - E_\alpha$	$E_\beta - E_\gamma$	$E_\alpha - E_\gamma$	Phase	Phase
KScGa	7.21	7.31	7.17	−1.54	−0.51	1.03	β	α
KTiGa	7.44	7.04	6.85	−1.73	−0.17	1.55	β	α
KVGa	7.47	7.14	7.07	−1.47	−0.20	1.27	β	α
KCrGa	7.58	7.24	7.17	−1.07	−0.07	1.00	β	α
KMnGa	7.44	7.12	6.96	−1.23	0.003	1.23	γ	α
KFeGa	7.39	6.95	6.80	−1.23	0.01	1.25	γ	α
KCoGa	7.29	6.85	6.60	−1.42	0.34	1.77	γ	α
KNiGa	7.12	6.75	6.63	−1.34	0.44	1.78	γ	α
KCuGa	7.40	7.02	6.95	−0.86	0.29	1.15	γ	α
KZnGa	7.64	7.26	7.23	−0.82	0.11	0.93	γ	α
KScGe	7.01	7.14	6.93	−2.07	−0.37	1.70	β	α
KTiGe	7.00	6.94	6.74	−2.30	−0.18	2.11	β	α
KVGe	7.12	6.92	6.66	−2.08	0.0001	2.08	γ	α
KCrGe	7.31	6.99	6.78	−1.62	0.03	1.65	γ	α
KMnGe	7.20	7.00	6.84	−1.80	−0.01	1.79	β	α
KFeGe	7.17	6.87	6.65	−1.76	0.15	1.91	γ	α
KCoGe	7.17	6.75	6.46	−1.87	0.39	2.25	γ	α
KNiGe	6.96	6.69	6.52	−1.72	0.55	2.27	γ	α
KCuGe	7.24	6.91	6.77	−1.33	0.38	1.70	γ	α
KZnGe	7.41	7.06	6.95	−1.38	0.16	1.53	γ	α

Table 1. *Cont.*

Compound	Lattice Constant a in Å			Energy Difference ΔE in eV			Most Stable Phase	Least Stable Phase
	α-Phase	β-Phase	γ-Phase	$E_\beta - E_\alpha$	$E_\beta - E_\gamma$	$E_\alpha - E_\gamma$		
KScAs	7.03	6.98	6.88	−2.39	−0.71	1.68	β	α
KTiAs	6.98	6.92	6.71	−2.48	−0.30	2.19	β	α
KVAs	6.99	6.85	6.66	−2.24	−0.14	2.10	β	α
KCrAs	7.10	6.93	6.74	−1.92	−0.07	1.85	β	α
KMnAs	7.08	6.92	6.75	−2.26	−0.12	2.15	β	α
KFeAs	7.09	6.80	6.60	−2.15	0.15	2.30	γ	α
KCoAs	7.03	6.76	6.51	−2.35	0.20	2.55	γ	α
KNiAs	6.94	6.70	6.47	−2.01	0.43	2.44	γ	α
KCuAs	7.27	6.82	6.63	−1.72	0.33	2.05	γ	α
KZnAs	7.29	6.88	6.74	−1.97	0.01	1.98	γ	α
KScSe	7.29	6.99	7.01	−2.00	−0.90	1.10	β	α
KTiSe	7.21	6.97	6.84	−2.01	−0.62	1.39	β	α
KVSe	7.14	6.97	6.80	−1.69	−0.26	1.43	β	α
KCrSe	7.19	7.03	6.86	−1.65	−0.20	1.45	β	α
KMnSe	7.32	7.03	6.76	−1.41	−0.22	1.19	β	α
KFeSe	7.11	6.87	6.57	−2.07	0.07	2.14	γ	α
KCoSe	7.07	6.76	6.50	−1.72	0.10	1.82	γ	α
KNiSe	7.02	6.75	6.51	−1.77	0.25	2.03	γ	α
KCuSe	7.12	6.84	6.61	−1.77	0.16	1.93	γ	α
KZnSe	7.36	7.25	7.09	−1.05	−0.19	0.85	β	α

In Table 1, we also present the total energy differences between the three phases, which were calculated at their respective equilibrium lattice constants. These energy differences are reported per formula unit in units of eV. A negative value indicates that the phase corresponding to the first total energy is more stable than the other phase in the comparison. In the Li-based compounds studied in Reference [30], the β phase was generally the most stable for most compounds, while the γ phase became the ground state for those with heavier transition metals. The energy differences between the three phases were relatively small, with absolute values always below 1 eV. However, in the K-based compounds examined here, the energy differences between the α phase and the β/γ phases are significantly larger, exceeding 2 eV in many cases, as shown in Table 1. Consequently, the α phase—where each K atom is at the center of a cube surrounded by four transition metal atoms and four sp atoms as nearest neighbors—emerges as the least stable phase across all forty compounds. In contrast, the energy difference between the β and γ phases remains small, and is consistently less than 1 eV. Generally, the β phase tends to be the ground state for lighter transition metals, while the γ phase becomes the ground state for heavier transition metals, with both phases being nearly degenerated for intermediate cases.

3.2. Electronic Properties

For all forty compounds in our study and across all three phases, we conducted electronic band structure calculations at the equilibrium lattice constants and subsequently extracted the total density of states (DOS) per formula unit (f.u.). The results for the KZGa and KZGe compounds are shown in Figure 1, while those for the KZAs and KZSe compounds are presented in Figure 2. To ensure clarity, we have chosen to display the DOS in the energy range of −5 eV to 2 eV for all compounds, with the vertical DOS axis ranging from −4.5 to 4.5 states per eV per spin per f.u. This standardization facilitates comparison between different compounds. Additionally, there is a small DOS contribution in both spin directions below the energy range shown in Figures 1 and 2, originating from the s states of the K atoms.

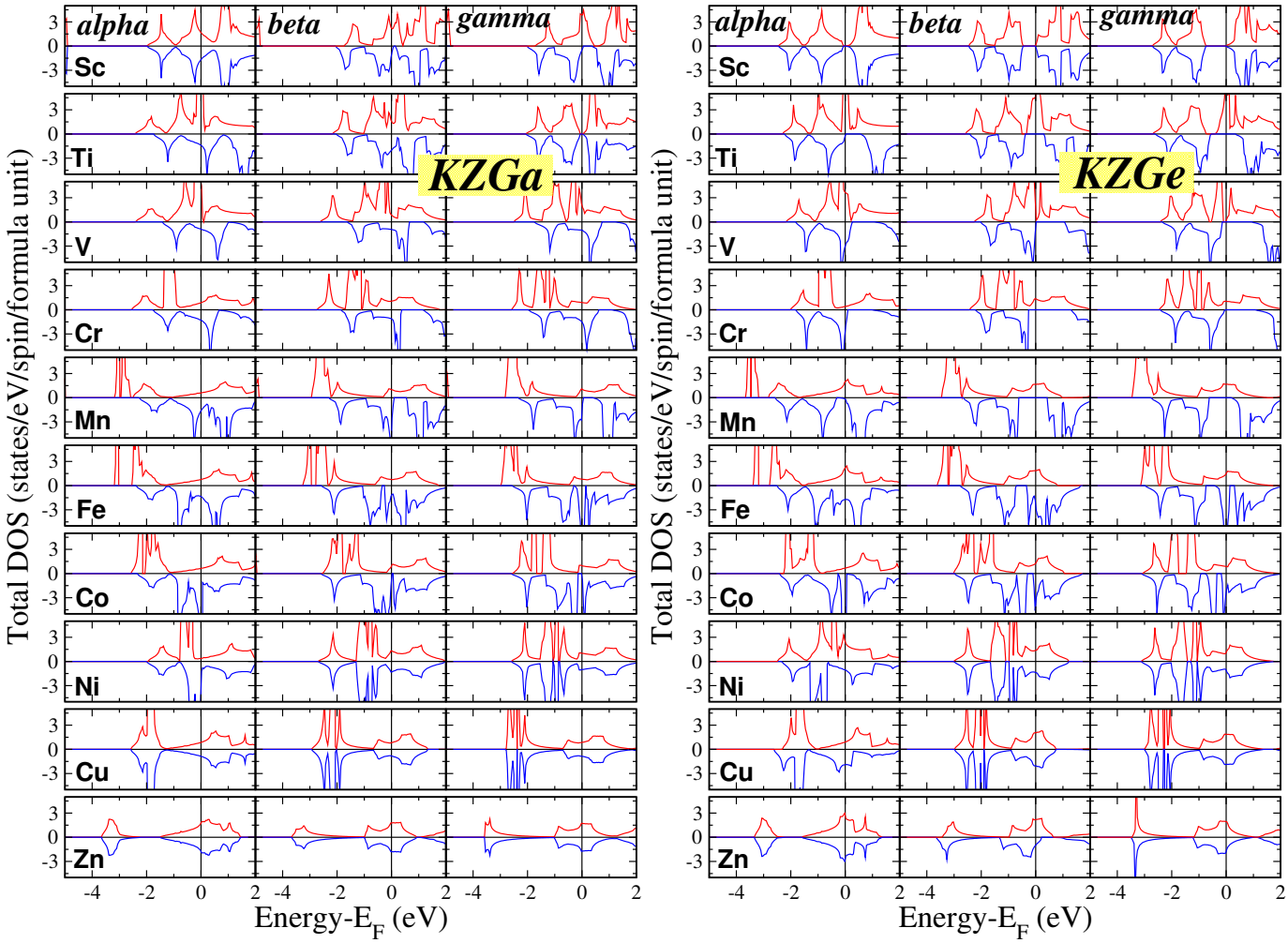

Figure 1. Total density of states (DOS) for the KZGa (**left** panel) and KZGe (**right** panel) compounds for all three phases. The zero energy has been assigned to the Fermi level. Positive (Negative) DOS values correspond to the spin-up (spin-down) electrons.

The general characteristics of the DOS are comparable to those observed in the Li compounds discussed in Reference [30]. The DOS presented in the figures is primarily due to the *p*-*d* hybridization between the *p*-states of the Ga/Ge/As/Se atoms and the *d*-states of the transition metal atoms. In the context of tetrahedral symmetry, the *d*-states split into two subgroups: (a) the triple-degenerate t_{2g} states, which are symmetrically allowed to hybridize with the *p*-states of the Ga/Ge/As/Se atoms [36], forming hybrids that extend across both the transition metal and the Ga/Ge/As/Se atoms, and (b) the double-degenerate e_g *d*-states, which, due to symmetry restrictions, do not hybridize and remain localized at the transition metal atoms. When *Z* is one of the heavier elements like Cu or Zn, all valence 3*d* states are fully occupied. For these cases, the 3*d*-DOS for both spin directions is concentrated in a narrow, high-intensity peak located deep in energy (for Zn compounds, this peak is outside the energy range displayed in the figures).

In contrast to the Li compounds from Reference [30], the K-based semi-Heusler compounds exhibit predominantly magnetic behavior, as shown in Tables 2 and 3 and discussed further in the next subsection. Only a few of these compounds are non-magnetic metals or semiconductors, with the transition metal atoms being either Sc (the lightest transition metal considered) or Ni/Cu/Zn (the heaviest transition metals considered), where the 3*d* states are nearly or completely occupied. Many of the magnetic compounds studied are either perfect or almost half-metals, displaying metallic behavior for spin-up electrons and semiconducting behavior for spin-down electrons across all three phases: KTiGe, KMnGe,

KTiAs, KVAs, KCrAs, KMnAs, KTiSe, KVSe, and KCrSe. Some compounds exhibit (almost) half-metallic properties in only one or two of the three phases: KScGa, KCoGa, KVGe, KCrGe, KScAs, and KScSe. Among these, the compounds that are nearly half-metallic have total spin magnetic moments slightly below the ideal integer value, as will be discussed in the next subsection, and the Fermi level marginally crosses the band just below the spin-down energy gap.

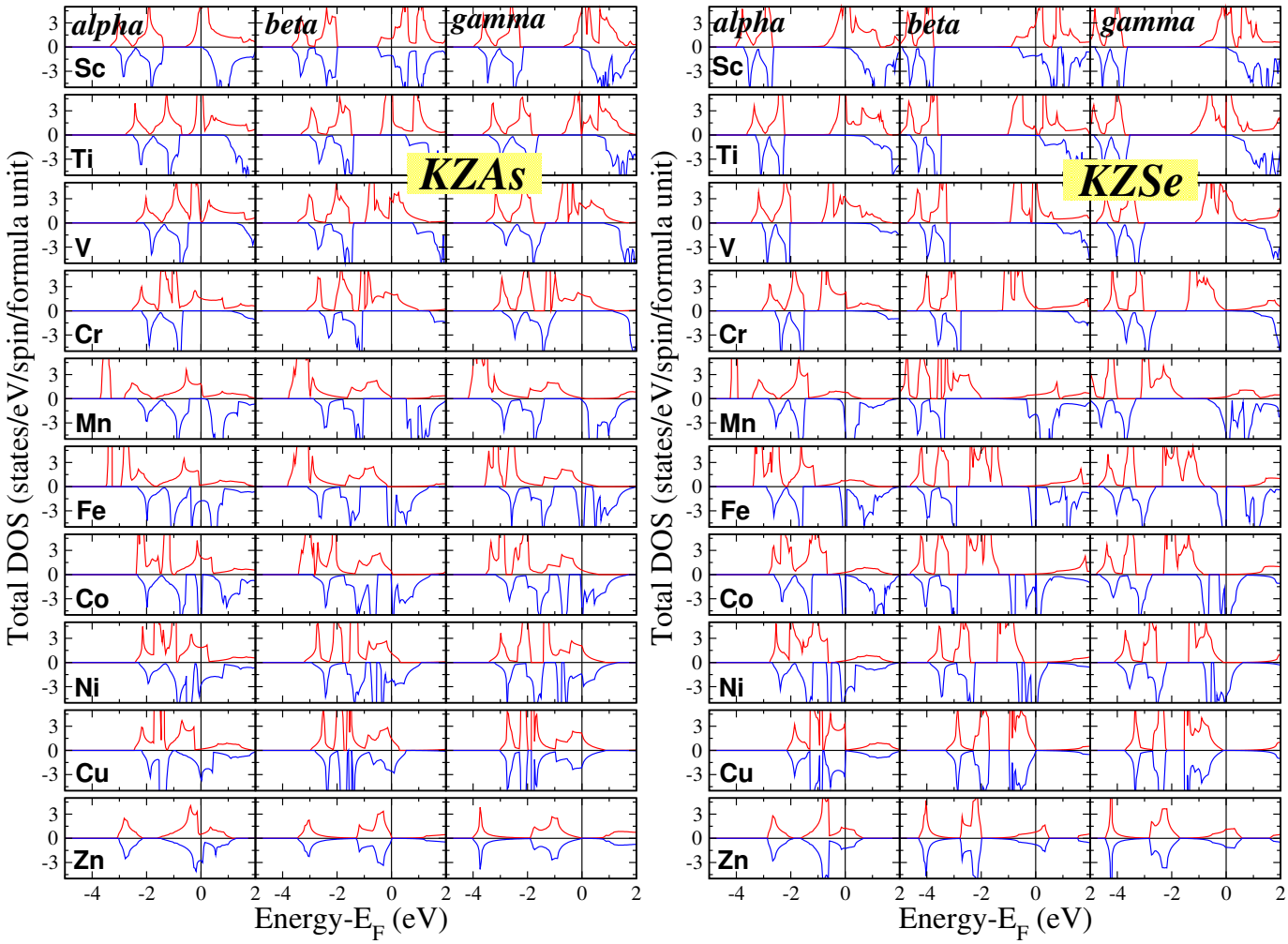

Figure 2. Similar to Figure 1 for the KZAs (**left** panel) and KZSe (**right** panel) compounds.

Table 2. For the KZGa and KZGe compounds, we provide the atom-resolved spin magnetic moments in μ_B units as well as the total spin magnetic moment m^{total} per formula unit that coincides with the per unit cell value. The last two columns are the total number of valence electrons in the unit cell, Z_t, as well as the ideal total spin magnetic moment if the Slater–Pauling rules were valid, m^{S-P}. For the non-magnetic compounds, we just present their electronic character.

Comp.	Phase	m^K	m^Z	m^{Ga}	m^{Total}	Z_t	m^{S-P}	Comp.	Phase	m^K	m^Z	m^{Ge}	m^{Total}	Z_t	m^{S-P}
KScGa	α	Metal				7	−1	KScGe	α	Gapless semiconductor				8	0
	β	0.031	−0.436	−0.523	−0.928	7	−1		β	Semiconductor				8	0
	γ	0.013	−0.537	−0.448	−0.972	7	−1		γ	Semiconductor				8	0
KTiGa	α	0.136	2.667	0.106	2.909	8	0	KTiGe	α	0.022	1.805	−0.827	1.000	9	1
	β	0.010	0.789	−0.096	0.703	8	0		β	0.108	1.374	−0.482	1.000	9	1
	γ	Gapless semiconductor				8	0		γ	0.032	1.339	−0.371	1.000	9	1
KVGa	α	0.168	4.146	0.301	4.615	9	1	KVGe	α	0.062	3.635	−0.797	2.900	10	2
	β	0.058	3.764	−0.448	4.270	9	1		β	0.091	2.937	−1.025	2.003	10	2
	γ	0.041	3.855	0.198	4.094	9	1		γ	0.023	2.828	−0.851	2.000	10	2

Table 2. *Cont.*

Comp.	Phase	m^K	m^Z	m^{Ga}	m^{Total}	Z_t	m^{S-P}	Comp.	Phase	m^K	m^Z	m^{Ge}	m^{Total}	Z_t	m^{S-P}
KCrGa	α	0.052	5.089	−0.261	4.880	10	2	KCrGe	α	0.007	4.991	−1.754	3.244	11	3
	β	−0.011	4.814	−0.052	4.751	10	2		β	0.110	4.438	−1.548	3.000	11	3
	γ	−0.011	4.851	−0.225	4.615	10	2		γ	0.034	4.280	−1.314	3.000	11	3
KMnGa	α	−0.086	4.624	−0.875	3.663	11	3	KMnGe	α	0.010	4.870	−0.912	3.968	12	4
	β	−0.078	4.492	−1.113	3.301	11	3		β	0.120	4.756	−0.876	4.000	12	4
	γ	−0.119	4.301	−1.092	3.090	11	3		γ	0.080	4.574	−0.654	4.000	12	4
KFeGa	α	−0.029	3.383	−0.399	2.955	12	4	KFeGe	α	−0.005	3.526	−0.481	3.040	13	5
	β	−0.023	3.311	−0.519	2.769	12	4		β	0.059	3.573	−0.145	3.487	13	5
	γ	−0.037	3.115	−0.566	2.512	12	4		γ	0.034	3.072	−0.593	2.513	13	5
KCoGa	α	−0.044	2.022	−0.281	1.697	13	5	KCoGe	α	−0.051	2.112	−1.484	0.577	14	6
	β	−0.060	1.765	−0.705	1.000	13	5		β	0.043	2.012	−0.643	1.412	14	6
	γ	−0.001	1.388	−0.387	1.000	13	5		γ	0.023	1.189	−0.337	0.875	14	6
KNiGa	α	−0.020	0.315	−0.159	0.136	14	6	KNiGe	α	0.024	−0.460	0.593	0.157	15	7
	β		Metal			14	6		β		Metal			15	7
	γ		Metal			14	6		γ		Metal			15	7
KCuGa	α		Metal			15	−3	KCuGe	α	−0.029	0.036	−1.112	−1.105	16	−2
	β		Metal			15	−3		β		Metal			16	−2
	γ		Metal			15	−3		γ		Metal			16	−2
KZnGa	α		Metal			16	−2	KZnGe	α		Metal			17	−1
	β		Metal			16	−2		β	0.016	−0.062	−0.695	−0.741	17	−1
	γ		Metal			16	−2		γ	−0.002	−0.015	−0.096	−0.103	17	−1

Table 3. Similar to Table 2 for the compounds where Z is As or Se.

Comp.	Phase	m^K	m^Z	m^{As}	m^{Total}	Z_t	m^{S-P}	Comp.	Phase	m^K	m^Z	m^{Se}	m^{Total}	Z_t	m^{S-P}
KScAs	α	0.050	1.146	−0.199	0.997	9	1	KScSe	α	0.090	1.920	−0.118	1.892	10	2
	β		Metal			9	1		β	0.072	0.674	−0.054	0.692	10	2
	γ	0.072	1.030	−0.133	0.969	9	1		γ	0.259	1.793	−0.118	1.934	10	2
KTiAs	α	0.044	2.371	−0.415	2.000	10	2	KTiSe	α	0.096	3.062	−0.174	2.984	11	3
	β	0.140	2.193	−0.333	2.000	10	2		β	0.294	2.889	−0.230	2.953	11	3
	γ	0.042	2.248	−0.290	2.000	10	2		γ	0.263	2.915	−0.193	2.985	11	3
KVAs	α	0.039	3.659	−0.698	3.000	11	3	KVSe	α	0.090	4.167	−0.698	4.000	12	4
	β	0.150	3.431	−0.581	3.000	11	3		β	0.252	4.014	−0.581	3.986	12	4
	γ	0.092	3.461	−0.553	3.000	11	3		γ	0.236	4.018	−0.553	4.000	12	4
KCrAs	α	0.028	4.988	−1.016	4.000	12	4	KCrse	α	0.042	5.200	−1.016	5.000	13	5
	β	0.104	4.652	−0.756	4.000	12	4		β	0.132	5.097	−0.756	4.997	13	5
	γ	0.071	4.582	−0.653	4.000	12	4		γ	0.137	5.060	−0.653	5.000	13	5
KMnAs	α	0.057	4.963	−0.020	5.000	13	5	KMnSe	α	0.039	5.306	−0.020	5.572	14	6
	β	0.094	4.911	−0.005	5.000	13	5		β	−0.034	4.290	−0.005	3.940	14	6
	γ	0.123	4.801	0.064	4.988	13	5		γ	0.089	4.054	0.035	3.717	14	6
KFeAs	α	0.018	3.641	0.477	4.136	14	6	KFeSe	α	0.004	3.678	−0.048	3.717	15	7
	β	0.032	3.699	0.269	4.000	14	6		β	0.006	3.154	−0.011	3.112	15	7
	γ	0.070	3.486	0.151	3.707	14	6		γ	0.033	2.985	0.151	3.007	15	7
KCoAs	α	−0.007	2.189	−0.712	3.717	15	7	KCoSe	α	−0.004	2.167	−0.004	2.158	16	8
	β	0.055	2.519	0.412	3.112	15	7		β	−0.049	2.046	0.075	2.072	16	8
	γ	0.078	2.252	0.371	3.007	15	7		γ	0.005	1.893	0.106	2.004	16	8
KNiAs	α	0.001	0.840	0.188	1.029	16	8	KNiSe	α	−0.010	0.947	0.170	1.107	17	9
	β	0.022	1.017	0.528	1.567	16	8		β	−0.014	0.900	0.122	1.008	17	9
	γ	0.029	0.645	0.382	1.056	16	8		γ	0.006	0.827	0.167	1.000	17	9
KCuAs	α	−0.004	0.060	−1.132	−1.076	17	−1	KCuSe	α		Gapless semiconductor			18	0
	β	−0.001	−0.081	−0.423	0.505	17	−1		β		Semiconductor			18	0
	γ		Metal			17	−1		γ		Semiconductor			18	0
KZnAs	α	0.001	−0.020	0.324	0.305	18	0	KZnSe	α		Metal			19	1
	β		Semiconductor			18	0		β		Metal			19	1
	γ		Semiconductor			18	0		γ		Metal			19	1

Examining the key characteristics of the total DOS for all forty compounds in this study, it is evident that the total DOS for the β and γ phases generally exhibits a similar shape, while the DOS for the α phase displays a distinct behavior. This difference can be attributed to symmetry considerations. In the β and γ phases, the Z and Ga/Ge/As/Se atoms are nearest neighbors, leading to similar bonding interactions and, consequently, similar DOS profiles for these phases. In contrast, in the α phase, these atoms are next-nearest neighbors, resulting in significantly weaker orbital interactions. This weaker interaction helps explain why the α phase is the least stable, as indicated in Table 1.

3.3. Magnetic Properties

Most of the compounds in this study are magnetic, and Tables 2 and 3 present the atomic and total spin magnetic moments calculated at their equilibrium lattice constants. For non-magnetic compounds, we provide their electronic classification as either metal, semiconductor, or gapless semiconductor (where the energy gap is negligible). The K atoms generally contribute negligible spin magnetic moments, with a few exceptions, notably when the metalloid is Se, the heaviest atom. As anticipated, the spin magnetic moments are primarily located at the transition metal atoms. However, due to the strong Ga/Ge/As/Se-p–Z-t_{2g} hybridization, significant induced spin magnetic moments are also present on the Ga/Ge/As/Se atoms. For most compounds, these induced moments are antiparallel to the spin magnetic moments of the transition metal atoms. For KScGa, KCuGe, KZnGe, and KCuAs, we have adjusted the signs of the atomic spin magnetic moments to ensure that the total spin magnetic moment is negative. This adjustment is made to maintain consistency with the Slater–Pauling rule, as discussed below.

Next, we focus on the total spin magnetic moment M_t per formula unit. Tables 2 and 3 display also the total number of valence electrons per unit cell (equivalent to the per formula unit value), Z_t, and the total spin magnetic moment predicted by the Slater–Pauling rule, which will be discussed in the following paragraph. All total spin magnetic moments are reported in μ_B units. Figure 3 illustrates the total spin magnetic moment as a function of the transition metal atom Z for all four families of compounds under study and for all three phases. The black dashed line represents the Slater–Pauling rule. Magnetic compounds that align with this rule and thus exhibit integer values of their total spin magnetic moments are identified as half-metallic ferromagnets, which is consistent with their total DOS discussed earlier. In contrast to the Li-based p^0-d compounds studied in Reference [30], the K-based d^0-d compounds examined here display half-metallic behavior in several cases, particularly when the metalloid atom is Ge, As, or Se, and the transition metal atom is Ti, V, Cr, or Mn. When the number of valence electrons, as noted in Tables 2 and 3, equals or exceeds 14, achieving half-metallicity would necessitate a total spin magnetic moment of 6 μ_B or more. Such values are energetically unfavorable, leading to the loss of half-metallicity, and the compounds remain merely magnetic. Compounds that exhibit half-metallic behavior across all three phases are especially promising for spintronic and magnetoelectronic applications.

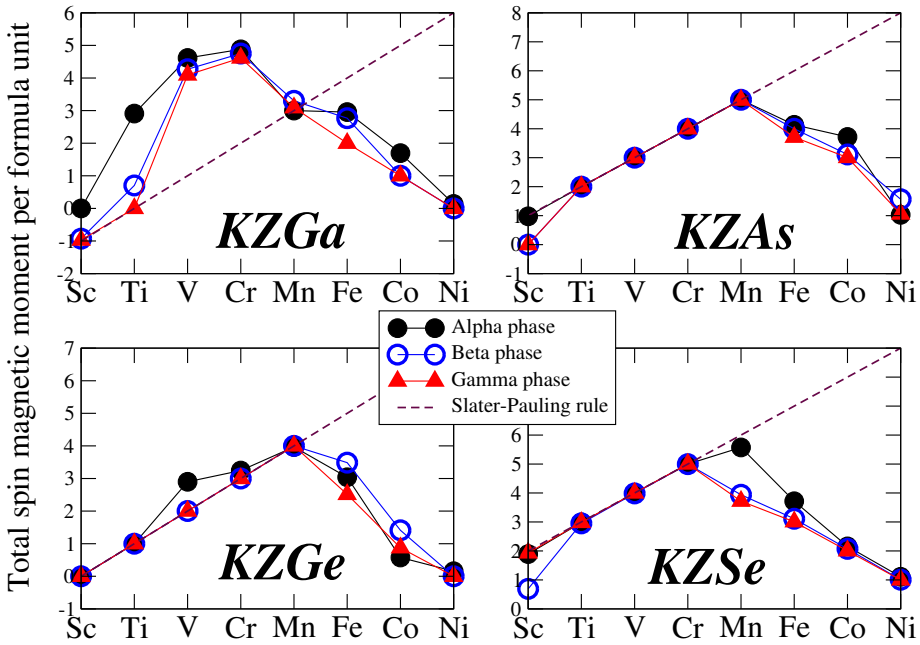

Figure 3. Total spin magnetic per formula unit in μ_B units as a function of the Z chemical element (Z = Sc $\rightarrow$ Ni) for all four studied families of K-based compounds. The black dashed lines represent the ideal Slater–Pauling rules for half-metallicity: $M_t = Z_t - 8$.

The explanation for the origin of half-metallicity follows the same reasoning as that for the Li-based semi-Heuslers discussed in Reference [30]. Here, we will briefly summarize it for completeness. When Z ranges from Sc to Ni and in the case of half-metallicity, the spin-down electronic band structure reveals exactly four fully occupied states. A low-energy s valence state from the K atom lies low in energy. The gap arises due to the hybridization of the p-t_{2g} states between the Ga/Ge/As/Se and the Z atoms. This leads to three bonding hybrids below the gap which are fully occupied, and three above the gap which are empty. The total spin magnetic moment corresponds to the number of uncompensated spins. For half-metallicity to be achieved, the total spin magnetic moment in the unit cell should adhere to the Slater–Pauling rule: $M_t = Z_t - 2 \times 4 = Z_t - 8$. When Z is Cu or Zn, all d valence states of the transition metal atoms are filled. In this case, the rule adjusts to $M_t = Z_t - 2 \times 9 = Z_t - 18$, provided half-metallicity is present.

4. Summary and Conclusions

Half-metallic semi-Heusler compounds are a prominent area of research due to their potential applications in spintronic devices. In the case of semi-Heusler compounds, there are three distinct variations of the $C1_b$ lattice structure—α, β, and γ—each with a different atomic arrangement within the unit cell. Using first-principles electronic band structure calculations, we investigate the KZ(Ga,Ge,As, or Se) d^0-d Heusler compounds, with Z ranging from Sc to Zn. Our study examines the structural, electronic, and magnetic properties of these compounds across the three $C1_b$ phases. We find that the β and γ phases are favored, while the α phase is consistently the least stable. This behavior is attributed to the variations in local environment and symmetry in each phase. Most of the compounds under study are magnetic and exhibit half-metallicity, in line with the Slater–Pauling rule regarding their total spin magnetic moment. Notably, compounds such as KTiGe, KMnGe, KTiAs, KVAs, KCrAs, KMnAs, KTiSe, KVSe, and KCrSe demonstrate (almost) half-metallic ferromagnetism across all three phases, highlighting their potential for practical applications.

We anticipate that our results will stimulate further experimental and theoretical research on these compounds, which hold significant potential for advancements in spintronics and magnetoelectronics.

Author Contributions: Both authors have equally contributed to all stages of the present study and manuscript preparation. All authors have read and agreed to the published version of the manuscript.

Funding: This research received no external funding

Data Availability Statement: The data presented in this study are available on request from the corresponding author.

Conflicts of Interest: The authors declare no conflicts of interest.

Abbreviations

The following abbreviations are used in this manuscript:

DOS	Density of states
f.u.	Formula unit
FPLO	Full-potential nonorthogonal local-orbital minimum- basis band structure approach
GGA	Generalized gradient approximation
PBE	Perdew–Burke–Ernzerhof

References

1. Heusler, F. Über magnetische manganlegierungen. *Verh. Dtsch. Phys. Ges.* **1903**, *12*, 219.
2. Heusler, F.; Take, E. The nature of the Heusler alloys. *Phys. Z.* **1912**, *13*, 897. [CrossRef]
3. Webster, P.J.; Ziebeck., K.R.A. Alloys and Compounds of *d*-Elements with Main Group Elements. Part 2. In *Landolt-Börnstein*; Wijn, H.R.J., Ed.; New Series, Group III, Vol 19c; Springer: Berlin/Heidelberg, Germany, 1988; pp. 75–184.

4. Ziebeck, K.R.A.; Neumann, K.-U. Magnetic Properties of Metals. In *Landolt-Börnstein*; Wijn, H.R.J., Ed.; New Series, Group III, Vol 32/c; Springer: Berlin/Heidelberg, Germany, 2001; pp. 64–414.
5. Kawasaki, J.K.; Chatterjee, S.; Canfield, P.C. Full and half-Heusler compounds. *MRS Bull.* **2022**, *47*, 555. [CrossRef]
6. Graf, T.; Felser, C.; Parkin, S.S.P. Simple rules for the understanding of Heusler compounds. *Prog. InSolid State Chem.* **2011**, *39*, 1. [CrossRef]
7. Bachagha, T; Sunol, J.-J. All-*d*-Metal Heusler Alloys: A Review. *Metals* **2023**, *13*, 111. [CrossRef]
8. de Paula, V.G.; Reis, M.S. All-*d*-Metal Full Heusler Alloys: A Novel Class of Functional Materials. *Chem. Mater.* **2021**, *33*, 5483. [CrossRef]
9. Tas, M; Özdoğan, K.; Şaşıoğlu, E.; Galanakis, I. High Spin Magnetic Moments in All-3d-Metallic Co-Based Full Heusler Compounds. *Materials* **2023**, *16*, 7543. [CrossRef]
10. Fortunato, N.M.; Li, X.; Schönecker, S.; Xie, R.; Taubel, A.; Scheibel, F.; Opahle, I.; Gutfleisch, O.; Zhang, H. High-Throughput Screening of All-d-Metal Heusler Alloys for Magnetocaloric Applications. *Chem. Mater.* **2024**, *36*, 6765. [CrossRef]
11. Galanakis, I. Slater–Pauling Behavior in Half-Metallic Heusler Compounds. *Nanomaterials* **2023**, *13*, 2010. [CrossRef]
12. Katsnelson, M.I.; Irkhin, V.Y.; Chioncel, L.; Lichtenstein, A.I.; de Groot, R.A. Half-metallic ferromagnets: From band structure to many-body effects. *Rev. Mod. Phys.* **2008**, *80*, 315. [CrossRef]
13. Hirohata, A.; Takanashi, K. Perspectives of Heusler compounds. *J. Phys. D Appl. Phys.* **2014**, *47*, 193001. [CrossRef]
14. Editors Felser, C.; Fecher, G.H. (Eds.) *Spintronics: From Materials to Devices*; Springer: Berlin/Heidelberg, Germany, 2013.
15. Fong, C.Y.; Pask, J.E.; Yang, L.H. (Eds.) Half-metallic Materials and Their Properties. In *Series on Materials for Engineering*; Imperial College Press: London, UK, 2013; Volume 2.
16. Felser, C.; Hirohata, A. (Eds.) Heusler Alloys. Properties, Growth, Applications. In *Springer Series in Materials Science*; Springer International Publishing: Cham, Switzerland, 2018; Volume 222.
17. Galanakis, I.; Özdoğan, K.; Şaşıoğlu, E. Spin-filter and spin-gapless semiconductors: The case of Heusler compounds. *AIP Adv.* **2016**, *6*, 055606. [CrossRef]
18. Gillessen, M.; Dronskowski, R. A combinatorial study of full Heusler alloys by first-principles computational methods. *J. Comput. Chem.* **2009**, *30*, 1290. [CrossRef] [PubMed]
19. Gillessen, M.; Dronskowski, R. A combinatorial study of inverse Heusler alloys by first-principles computational methods. *J. Comput. Chem.* **2010**, *31*, 612. [CrossRef] [PubMed]
20. Ma, J.; Hegde, V.I.; Munira, K.; Xie, Y.; Keshavarz, S.; Mildebrath, D.T.; Wolverton, C.; Ghosh, A.W.; Butler, W.H. Computational investigation of half-Heusler compounds for spintronics applications. *Phys. Rev. B* **2017**, *95*, 024411. [CrossRef]
21. Sanvito, S.; Oses, C.; Xue, J.; Tiwari, A.; Zic, M.; Archer, T.; Tozman, P.; Venkatesan, M.; Coey, M.; Curtarolo, S. Accelerated discovery of new magnets in the Heusler alloy family. *Sci. Adv.* **2017**, *3*, e1602241. [CrossRef]
22. Faleev, S.V.; Ferrante, Y.; Jeong, J.; Samant, M.G.; Jones, B.; Parkin, S.S.P. Unified explanation of chemical ordering, the Slater-Pauling rule, and half-metallicity in full Heusler compounds. *Phys. Rev. B* **2017**, *95*, 045140. [CrossRef]
23. Faleev, S.V.; Ferrante, Y.; Jeong, J.; Samant, M.G.; Jones, B.; Parkin, S.S.P. Heusler compounds with perpendicular magnetic anisotropy and large tunneling magnetoresistance. *Phys. Rev. Mater.* **2017**, *1*, 024402. [CrossRef]
24. He, J.; Rabe, K.M.; Wolverton, C. Computationally accelerated discovery of functional and structural Heusler materials. *MRS Bull.* **2022**, *47*, 559. [CrossRef]
25. Damewood, L.; Busemeyer, B.; Shaughnessy, M.; Fong, C.Y.; Yang, L.H.; Felser, C. Stabilizing and increasing the magnetic moment of half-metals: The role of Li in half-Heusler LiMnZ (Z = N, P, Si). *Phys. Rev. B* **2015**, *91*, 064409. [CrossRef]
26. Dehghan, A.; Davatolhagh, S. d^0-*d* half-Heusler alloys: A potential class of advanced spintronic materials. *J. All. Compd.* **2019**, *773*, 132. [CrossRef]
27. Shakil, M.; Kousar, M.; Gillani, S.S.A.; Rizwan, M.; Arshad, H.; Rafique, M.; Zafar, M. First principle computation of half metallicity and mechanical properties of a new series of half Heusler alloys KMnZ (Z = B, Si, Ge, As) for spintronics. *Ind. J. Phys.* **2022**, *96*, 115–126. [CrossRef]
28. Dehghan, A.; Davatolhagh, S. First principles study of d^0-*d* half-Heusler alloys containing group-IV, -V, and -VI sp atoms as prospective half-metals for real spintronic applications. *Mater. Chem. Phys.* **2021**, *273*, 125064. [CrossRef]
29. Javari, A.R.; Davatolhagh, S.; Dehghan, A. Half-metallic p^0-*d* half-Heusler alloys with stable structure in ferromagnetic state. *J. Phys. Chem. Solids* **2022**, *166*, 110702. [CrossRef]
30. Özdoğan, K.; Galanakis, I. Interplay between Structural, Electronic, and Magnetic Properties in the p^0-*d* Semi-Heusler Compounds: The Case of Li-Based Compounds. *Crystals* **2024**, *14*, 693. [CrossRef]
31. Koepernik, K.; Eschrig, H. Full-potential nonorthogonal local-orbital minimum-basis band-structure scheme. *Phys. Rev. B* **1999**, *59*, 1743. [CrossRef]
32. Kopernik, K. Full Potential Local Orbital Minimum Basis Bandstructure Scheme User's Manual. Available online: http://www.fplo.de/download/doc.pdf (accessed on 1 September 2024).
33. Perdew, J.P.; Burke, K.; Ernzerhof, M. Generalized Gradient Approximation Made Simple. *Phys. Rev. Lett.* **1996**, *77*, 3865. [CrossRef]
34. Meinert, M. Modified Becke-Johnson potential investigation of half-metallic Heusler compounds. *Phys. Rev. B* **2013**, *87*, 045103. [CrossRef]

35. Lompwsky, L.; Bronger, W. Synthese und Kristallstruktur von KMnP und KMnAs. *Z. Anorg. Allg. Chem.* **1974**, *409*, 221–227. [CrossRef]
36. Harrison, W.A. *Electronic Structure and the Properties of Solids: The Physics of the Chemical Bond*; Dover: Mineola, NY, USA, 1989.